

Supporting Information:

Donor-acceptor interactions of gold(III) porphyrins with cobalt(II) phthalocyanine: chemical structure of products, their spectral characterization and DFT study

Nataliya Bichan,^a Arshak Tsaturyan,^{b,c*} Ekaterina Ovchenkova,^a Nadezhda Kudryakova,^a Fedor Gostev,^d Ivan Shelaev,^d Arseny Aybush,^d Victor Nadtochenko^{d,e} and Tatyana Lomova^a

^aG.A. Krestov Institute of Solution Chemistry of the Russian Academy of Sciences,
Akademicheskaya Str. 1, Ivanovo, Russia

^b Univ Lyon, UJM-Saint-Etienne, CNRS, IOGS, Laboratoire Hubert Curien UMR5516, F-42023
St-Etienne, France

^cInstitute of Physical and Organic Chemistry, Southern Federal University, Stachki Av. 194/2
Rostov-on-Don, Russia

^dSemenov Institute of Chemical Physics of the Russian Academy of Sciences, Kosigin Str. 4,
Moscow, Russia

^eLomonosov Moscow State University, Faculty of Chemistry, Leninskie Gory 1, Moscow, Russia
Corresponding author: arshak.tsaturyan@univ-st-etienne.fr

(2,3,7,8,12,18-hexamethyl,13,17-diethyl,5-(pyridine-4-yl)porphinato)gold(III) chloride, 2	3
Figure S1. ¹ H NMR spectrum in CDCl ₃ (a) and MALDI-TOF mass spectrum (b) of 2	3
(2,3,7,8,12,18-hexamethyl,13,17-diethyl,5-(pyridine-3-yl)porphinato)gold(III) chloride, 3	4
Figure S2. ¹ H NMR spectrum in CDCl ₃ (a) and MALDI-TOF mass spectrum (b) of 3	5
(Octakis(3,5-di- <i>tert</i> -butylphenoxy)phthalocyaninato)cobalt(II), 1	5
Figure S3. The MALDI-TOF mass spectrum of 1	6
Figure S4. The changes in the UV-vis spectrum of 1 in 1,2-dichlorobenzene during its reaction with 2 ($C_1 = 5.4 \times 10^{-6}$ M, $C_2 = 3.8 \times 10^{-5}$ M) for 6 h. Areas of preferential absorption of one of the complexes are highlighted in different colors	6
Figure S5. The changes in absorbance in the visible region of the electron spectrum during the titration of 1 with 3 ($C_3 = 1.0 \times 10^{-6} \div 1.2 \times 10^{-4}$ M) in 1,2- dichlorobenzene at $\tau = \infty$ and the corresponding spectrophotometric titration curves at 673 nm (a); the plots of an indicator ratio vs logC ₃ for the reactions of 1 with 3 at $\tau = \infty$ (b). Job's plot for 1:2 (c) and 1:3 (d) dyads in 1,2- dichlorobenzene at $\tau = \infty$; in Jobs experiment, the concentration of 1 and gold(III) porphyrins are continuously varied in the concentration range of 0.6×10^{-6} M to 1.21×10^{-5} M.	7
Table S1. The first-order rate constants, k_{obs} , and k (kinetic coefficient independent of any concentrations) for the reaction of 1 with 2 and 3 in 1,2- dichlorobenzene at 298 K	7
Figure S6. The spectrophotometric titration curves and the corresponding plots of logI vs logC _{AuP} for the reaction of 1 with 2 (a) and 3 at $\tau = 0$ (b).	8

Fig. S7. The IR spectra of 1 and its dyad with 3 in KBr. Bands corresponding to vibrations of 3 are denoted with asterisks	8
Table S2. The chemical shifts of protons of 1 and 1:2/1:3 dyad.....	9
Fig. S8. TG and DTG curves for 1 (<i>a</i>), 3 (<i>b</i>) and 1:3 (<i>c</i>) powder from 25 °C to 920 °C, heating rate of 10 °C/min.....	9
Table S3. The peak potentials for 3, 2, 1:3, 1:2 in CH ₂ Cl ₂ containing 0.1 M (n-Bu) ₄ NClO ₄	9
Figure S9. The selective bond lengths (Å) of 1, 2Cl, 3Cl. Hydrogen atoms are omitted for clarity	10
Figure S10. The selective bond lengths (Å) of 1:3Cl (<i>a</i>) and 1:2Cl (<i>b</i>). Hydrogen atoms are omitted for clarity	10
Table S4. Bond order analysis based on Mulliken, Mayer, and Laplacian bond order of 2, 3 compounds	11
Table S5. The conductivity and molar conductivity of 3 in CH ₂ Cl ₂	12
Figure S11. Energy diagrams of the frontier MO (alpha) levels and its shapes (Isodensity contour 0.03) for 1, 2Cl, 3Cl, 1:3Cl and 1:2Cl in toluene calculated using TD-UB3LYP*/6-31G (C, H, O, Cl) and Lanl2DZ (Co, Au) level of theory.....	13
Table S6. The selected calculated optical transitions of 1:3 with oscillator strengths f > 0.1, wavelengths (nm) and main orbital transition contributions (>10%) of HOMO, LUMO (A- alpha orbitals, B – beta orbitals). Contour value is 0.03	14
Table S7. The selected calculated optical transitions of 1:2 with oscillator strengths f > 0.1, wavelengths (nm) and main orbital transition contributions (>10%) of HOMO, LUMO. Contour value is 0.03	17
Table S8. The selected calculated electron transitions, Λ parameters values and Δr-index for 1:2 and 1:3 by using B3LYP/6-31G level of theory with oscillator strengths f > 0.05.....	23
Table S9. The Natural Transition Orbitals of 1:3 for electron excitation with oscillator strengths f > 0.1, wavelengths (nm) and main orbital transition contributions (>10%). A- alpha orbitals, B – beta orbitals. Contour value is 0.001	24
Table S10. The Natural Transition Orbitals of 1:2 for electron excitation with oscillator strengths f > 0.1, wavelengths (nm) and main orbital transition contributions (>10%). A- alpha orbitals, B – beta orbitals. Contour value is 0.001	26
Figure S12. The femtosecond transient absorption spectra of 1 at the excitation wavelength of 400 nm in argon saturated 1,2- dichlorobenzene at indicated time intervals.	28
Figure S13. The femtosecond transient absorption spectra of 2 at the excitation wavelength of 400 nm in argon saturated 1,2- dichlorobenzene at indicated time intervals.	28

(2,3,7,8,12,18-hexamethyl,13,17-diethyl,5-(pyridine-4-yl)porphinato)gold(III) chloride, 2

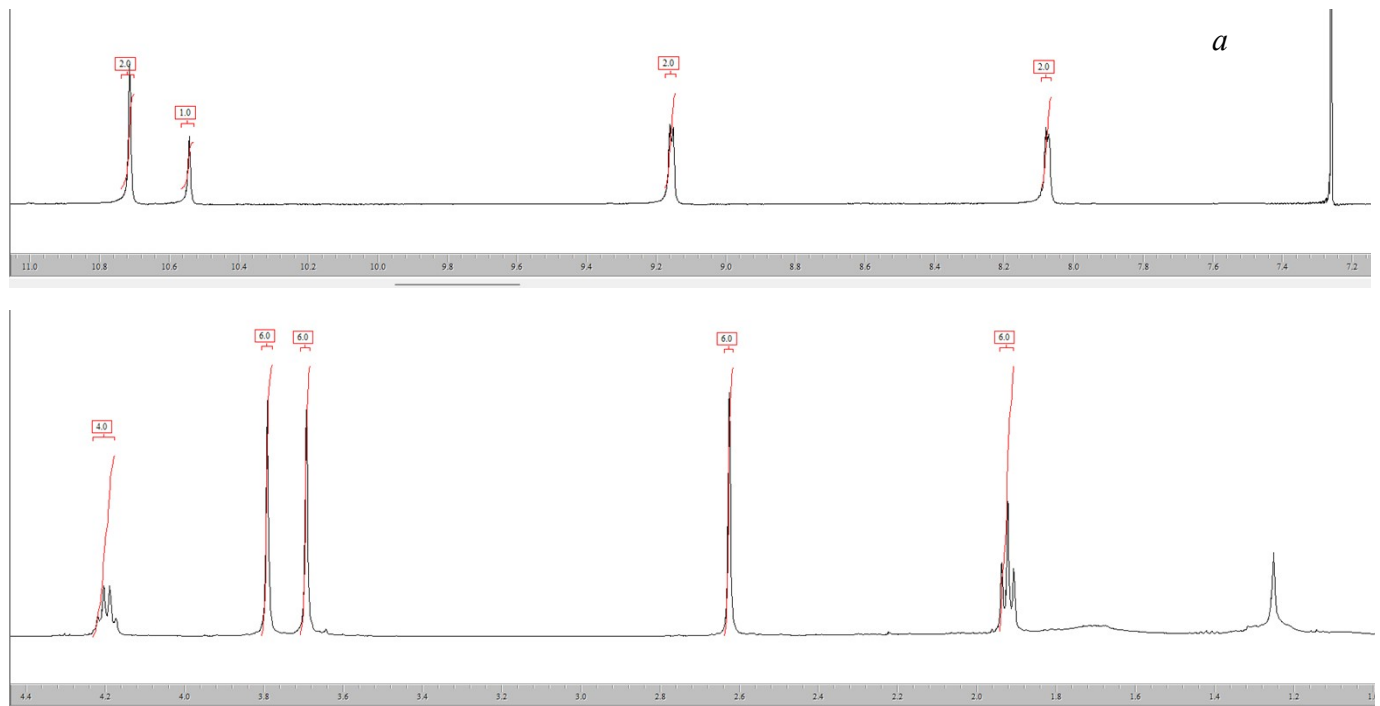
2 was synthesized by the reaction of (2,3,7,8,12,18-hexamethyl,13,17-diethyl,5-(4-pyridyl)porphyrin (30 mg, 0.057 mmol) with KAuCl_4 (107 mg, 0.28 mmol) in boiling acetic acid for 3 h. When the reaction was over, the contents of the reaction flask were cooled. The solvent was distilled off in vacuum. The reaction mixture was dissolved in dichloromethane. The solution in CH_2Cl_2 was repeatedly washed with distilled water to remove AcOH . The residual solution of the complex was purified by the chromatography on the Al_2O_3 column (grade II activity according to Brockman) using the mixture $\text{CH}_2\text{Cl}_2\text{-CH}_3\text{OH}$ (20:1) as the eluent. The AuP(4-py) yield is 80%. UV-vis (1,2-dichlorobenzene) λ_{\max} nm, ($\log \epsilon$): 398 (4.92), 515 (3.72), 551 (3.84). IR (KBr) ν , cm^{-1} : 3025 $\nu(\text{C-H})$; 2962 $\nu_{\text{as}}(-\text{CH}_3)$; 2924 $\nu_{\text{as}}(-\text{CH}_2-)$; 2852 $\nu_s(-\text{CH}_2-)$; 1721, 1691, 1593, 1547 vibrations of pyridyl group; 1446 $\delta(-\text{CH}_2-)$, 1385 $\delta_{\text{as}}(-\text{CH}_3)$; 1180 $\nu(\text{C-H})$ of pyridyl group; 1272, 1211, 1164, 1154, 1120, 1109, 1098, 1060 vibrations of macrocycle; 989, 954 vibrations of pyrrole groups; 852, 791, 759, 739 $\delta(\text{C-H})$ of pyridyl group; 717, 698, 645, 534 vibrations of macrocycle; 466 $\nu(\text{Au-N})$.

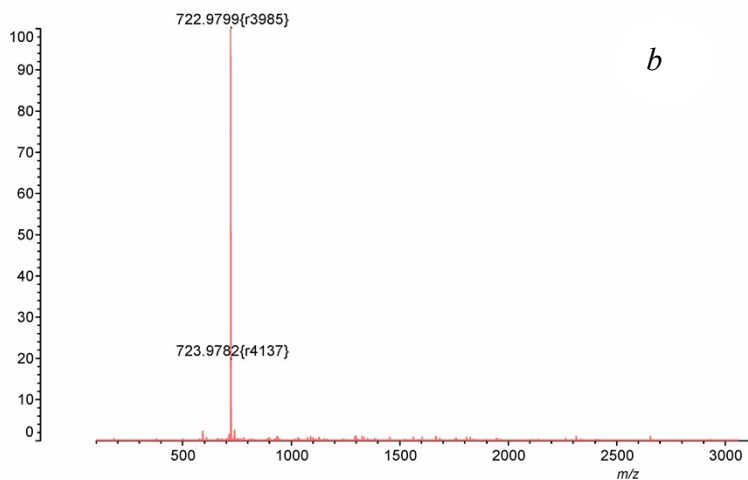
¹H NMR (CDCl_3) δ , ppm: 1.92 (t, 6H- CH_3 , $J = 7.42$ Hz), 2.63 (s, 6H- CH_3), 3.69 (s, 6H- CH_3), 3.79 (s, 6H- CH_3), 4.20 (q, 4H- CH_2- , $J = 7.77$ Hz), 8.08 (d, 2H-Py, $J = 4.95$ Hz), 9.16 (d, 2H-Py, $J = 4.95$ Hz), 10.54 (s, 1H_{meso}), 10.71 (s, 2H_{meso}).

¹³C NMR (CDCl_3) δ, ppm: 150.59, 147.95, 144.88, 140.93, 139.64, 138.53, 135.58, 134.86, 133.27, 128.81, 119.09, 101.43, 99.91, 20.87, 18.05, 17.18, 13.37, 12.73.

MS (MALDI-TOF) (*m/z*): found 722.9799 [M-Cl]⁺; calculated for C₃₅H₃₅AuN₅ 722.67.

Figure S1. ^1H NMR spectrum in CDCl_3 (a) and MALDI-TOF mass spectrum (b) of 2





(2,3,7,8,12,18-hexamethyl,13,17-diethyl,5-(pyridine-3-yl)porphinato)gold(III) chloride, 3

3 was synthesized by the reaction of (2,3,7,8,12,18-hexamethyl,13,17-diethyl,5-(3-pyridyl)porphyrin (40 mg. 0.076 mmol) with KAuCl_4 (143 mg. 0.38 mmol) in boiling acetic acid for 4 h. The isolation and purification of the complex were similar to $\text{AuP}(4\text{-py})$. The $\text{AuP}(3\text{-py})$ yield is 80%.

UV-vis (1,2-dichlorobenzene) λ_{\max} nm, ($\log \epsilon$): 398 (4.92), 515 (3.72), 551 (3.84).

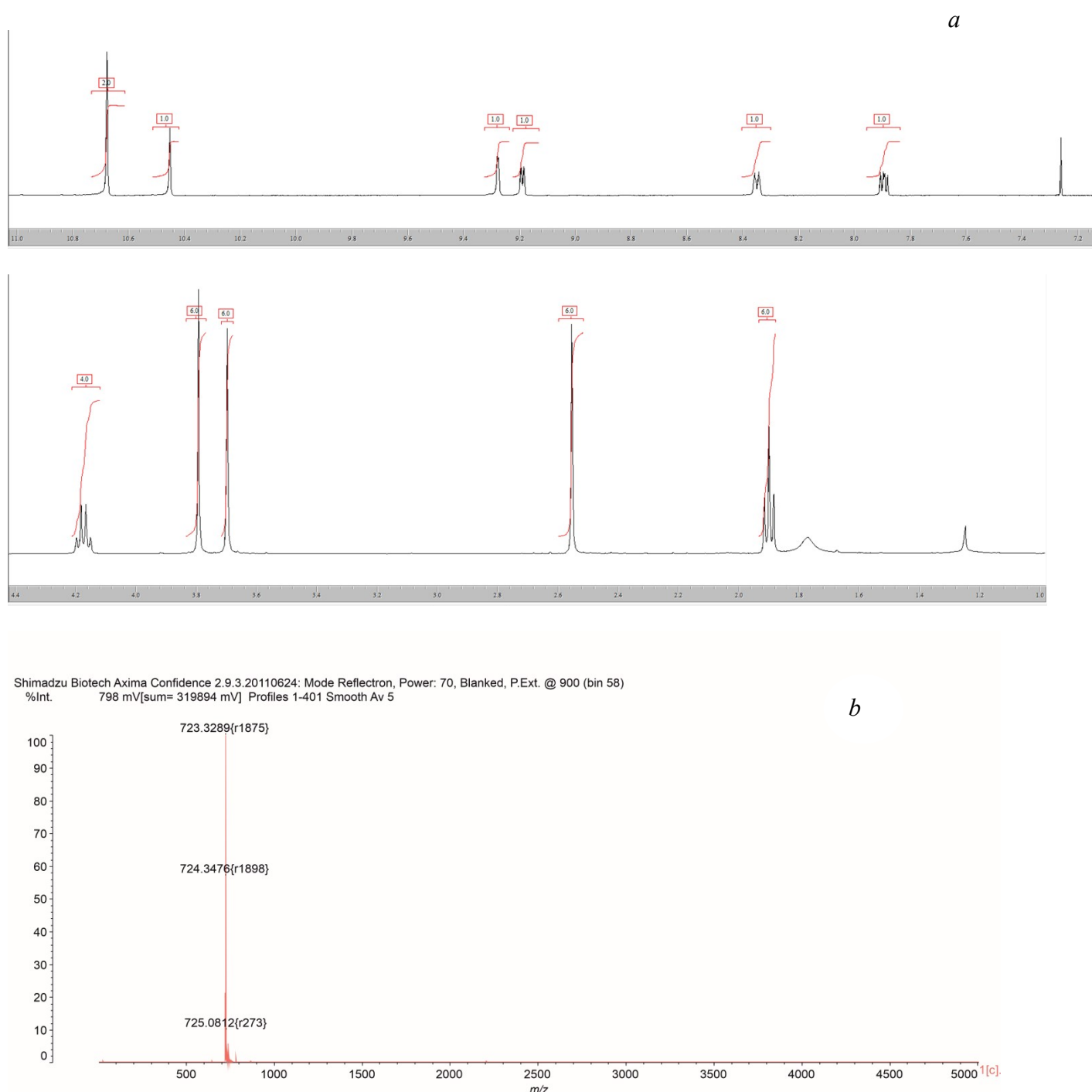
IR (KBr) ν , cm^{-1} : 3025 $\nu(\text{C-H})$; 2963 $\nu_{\text{as}}(-\text{CH}_3)$, 2925 $\nu_{\text{as}}(-\text{CH}_2-)$, 2854 $\nu_{\text{s}}(-\text{CH}_2-)$; 1719, 1691, 1588, 1566 vibrations of pyridyl group; 1445 $\delta(-\text{CH}_2-)$, 1385 $\delta_{\text{as}}(-\text{CH}_3)$; 1182 $\nu(\text{C-H})$ of pyridyl group; 1273, 1214, 1164, 1154, 1128, 1111, 1099, 1059 vibrations of macrocycle; 984, 955 vibrations of pyrrole groups; 846, 786, 760, 744 $\delta(\text{C-H})$ of pyridyl group; 717, 700, 645, 533 vibrations of macrocycle; 471 $\nu(\text{Au-N})$.

^1H NMR (CDCl_3) δ , ppm: 1.90 (t, 6H- CH_3 , $J = 7.77$ Hz), 2.55 (s, 6H- CH_3), 3.70 (s, 6H- CH_3), 3.79 (s, 6H- CH_3), 4.18 (q, 4H- CH_2- , $J = 7.77$ Hz), 7.90 (m, 1H_{Py}), 8.35 (d, 1H_{Py}, $J = 5.02$ Hz), 9.19 (d, 1H_{Py}, $J = 4.93$ Hz), 9.28 (s, 1H_{Py}), 10.45 (s, 1H_{meso}), 10.68 (s, 2H_{meso}).

^{13}C NMR (CDCl_3) δ , ppm: 152.42, 151.61, 144.71, 140.83, 199.93, 138.48, 136.28, 135.40, 134.74, 134.26, 124.37, 101.39, 99.73, 20.85, 18.05, 17.70, 13.37, 12.75.

MS (MALDI-TOF) (*m/z*): found 723.3289 [M-Cl^+]; calculated for $\text{C}_{35}\text{H}_{35}\text{AuN}_5$ 722.67.

Figure S2. ^1H NMR spectrum in CDCl_3 (*a*) and MALDI-TOF mass spectrum (*b*) of 3



(Octakis(3,5-di-*tert*-butylphenoxy)phthalocyaninato)cobalt(II), 1

UV-vis (1,2-dichlorobenzene), λ_{max} (log ϵ) nm: 305 (4.82), 336 (4.78), 611 (4.51), 677 (5.21). IR (KBr), ν , cm^{-1} : 2964, 2905, 2868 $\nu(\text{C-H})$ *tert*-butyl groups; 1608, 1588, 1524 benzene stretching; 1457, 1415 isoindole stretching; 1363, 1348 $\delta(\text{C-H})$ *tert*-butyl groups; 1246 $\nu(\text{C-C})$ *tert*-butyl groups; 1297, 1274, 1198, 1145, 1095, 1052, 961, 903, 864, 836, 756, 726, 707, 555, 463 vibrations of macrocycles; 439 $\nu(\text{Co-N})$. ^1H NMR (CDCl_3): 16.46 (s, 8 $\text{H}_{\text{isoindole}}$), 8.93 (s, 16 H_o), 8.02 (s, 8 H_p), 1.89 (s, 144 H_{tBu}) ppm. MALDI-TOF MS: found 2205.26 [$\text{M}]^+$, calculated for $\text{C}_{144}\text{H}_{176}\text{N}_8\text{O}_8\text{Co}$ – 2205.97 (Fig. S3†).

Figure S3. The MALDI-TOF mass spectrum of 1

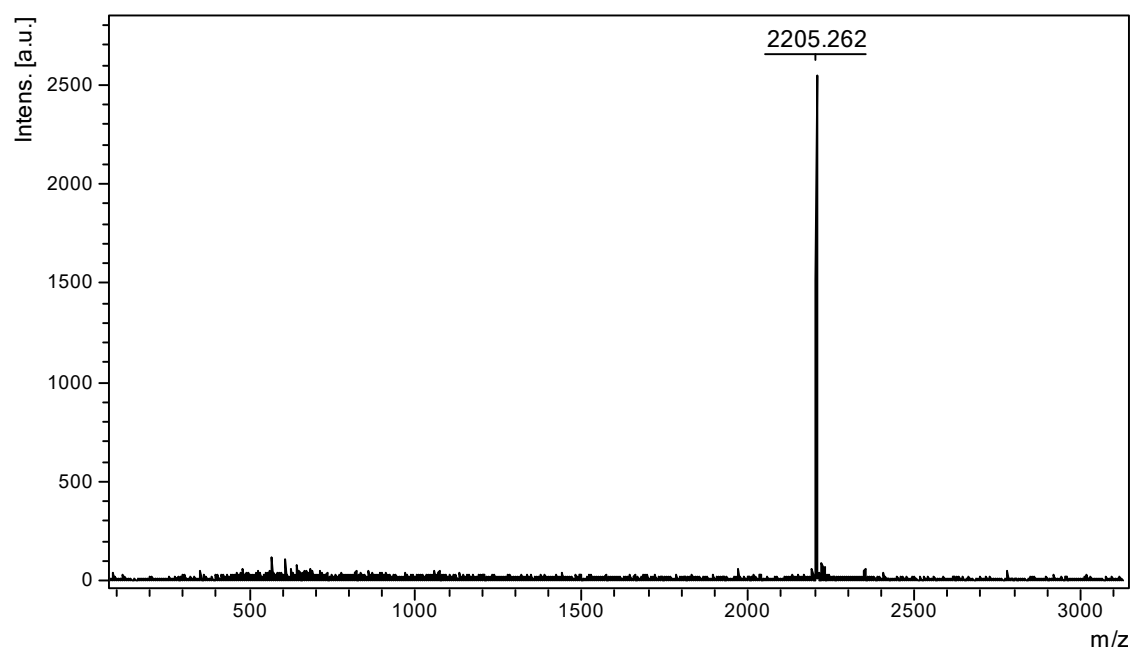


Figure S4. The changes in the UV-vis spectrum of 1 in 1,2-dichlorobenzene during its reaction with 2 ($C_1 = 5.4 \times 10^{-6}$ M, $C_2 = 3.8 \times 10^{-5}$ M) for 6 h. Areas of preferential absorption of one of the complexes are highlighted in different colors

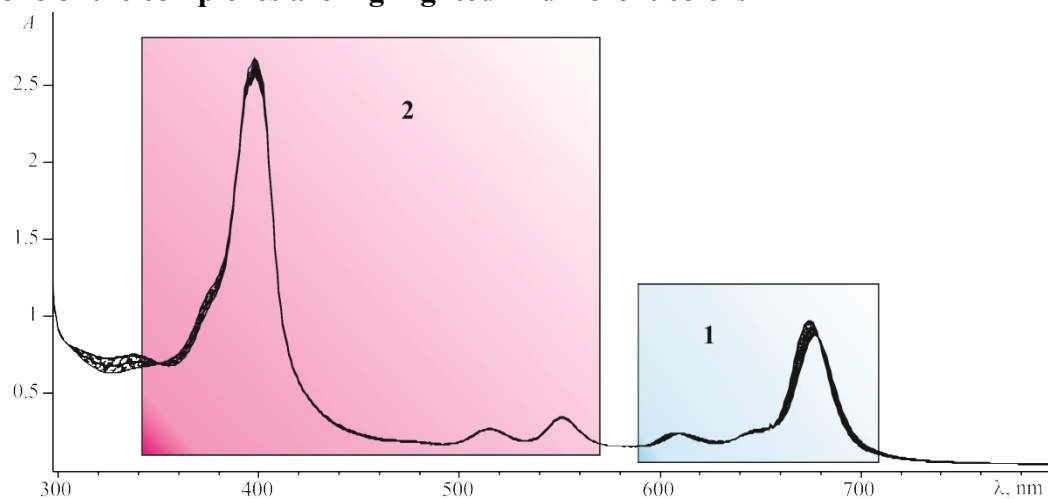


Figure S5. The changes in absorbance in the visible region of the electron spectrum during the titration of 1 with 3 ($C_3 = 1.0 \times 10^{-6} \div 1.2 \times 10^{-4}$ M) in 1,2-dichlorobenzene at $\tau = \infty$ and the corresponding spectrophotometric titration curves at 673 nm (a); the plots of an indicator ratio vs $\log C_3$ for the reactions of 1 with 3 at $\tau = \infty$ (b). Job's plot for 1:2 (c) and 1:3 (d) dyads in 1,2-dichlorobenzene at $\tau = \infty$; in Jobs experiment, the concentration of 1 and gold(III) porphyrins are continuously varied in the concentration range of 0.6×10^{-6} M to 1.21×10^{-5} M.

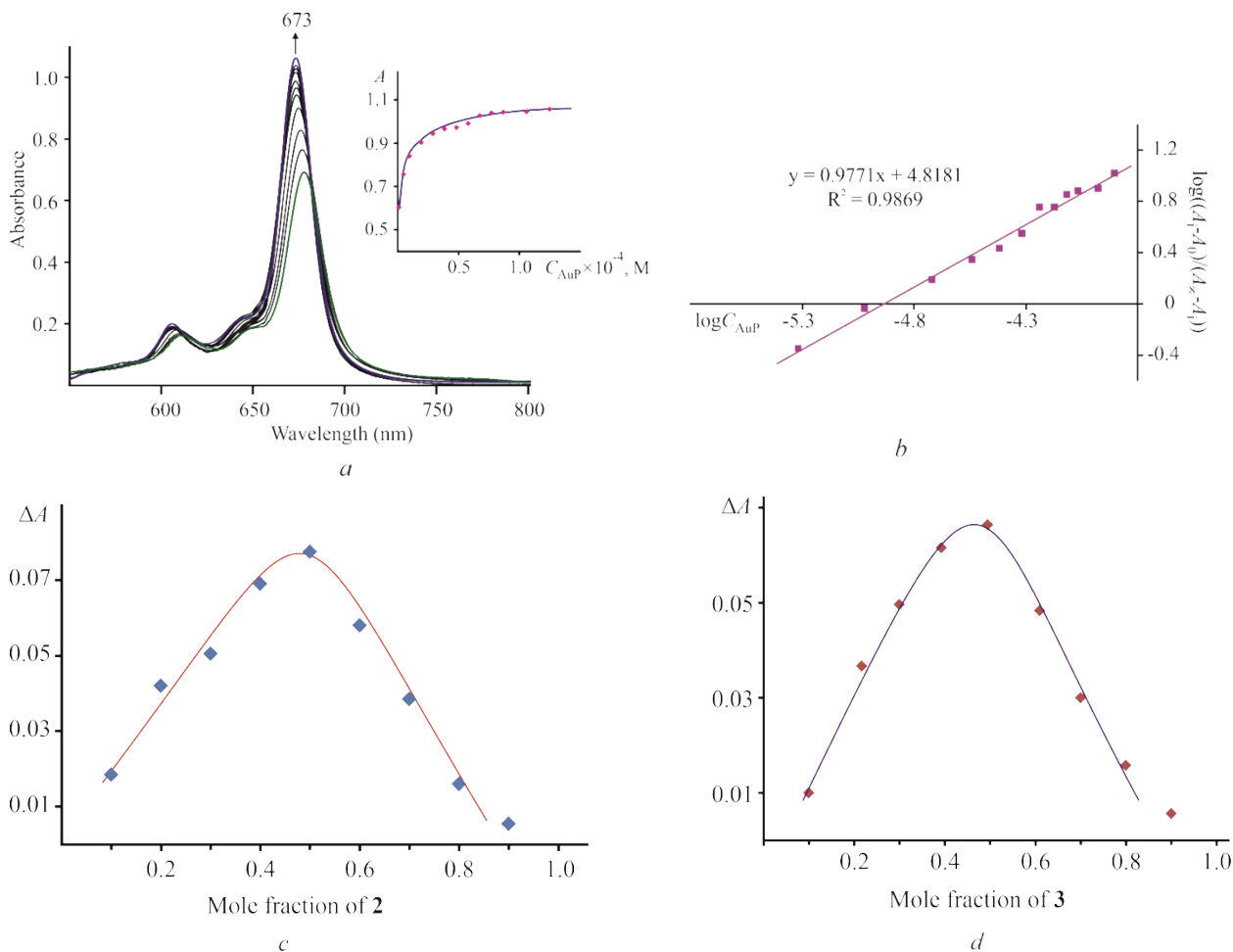


Table S1. The first-order rate constants, k_{obs} , and k (kinetic coefficient independent of any concentrations) for the reaction of 1 with 2 and 3 in 1,2-dichlorobenzene at 298 K

$C_2 \times 10^5 / \text{M}$	$(k_{\text{obs}} \pm \delta k_{\text{obs}}) \times 10^5 / \text{s}^{-1}$	$C_3 \times 10^5 / \text{M}$	$(k_{\text{obs}} \pm \delta k_{\text{obs}}) \times 10^5 / \text{s}^{-1}$
1.61	7.28 ± 0.49	2.90	6.39 ± 0.28
2.14	7.87 ± 0.51	3.86	6.05 ± 0.49
2.68	6.92 ± 0.6	4.83	6.76 ± 0.58
3.75	7.85 ± 0.58	5.79	6.44 ± 0.39
4.82	6.81 ± 0.61	6.76	6.70 ± 0.59
5.89	6.34 ± 0.59	7.72	6.32 ± 0.56
6.96	7.14 ± 0.59	8.69	6.72 ± 0.53
8.03	7.74 ± 0.42	10.60	6.84 ± 0.61
		12.50	6.02 ± 0.49
1.61 – 8.03	$k = 7.24 \pm 0.47$	2.90 – 12.50	$k = 6.14 \pm 0.44$

Figure S6. The spectrophotometric titration curves and the corresponding plots of $\log I$ vs $\log C_{\text{AuP}}$ for the reaction of 1 with 2 (a) and 3 at $\tau = 0$ (b).

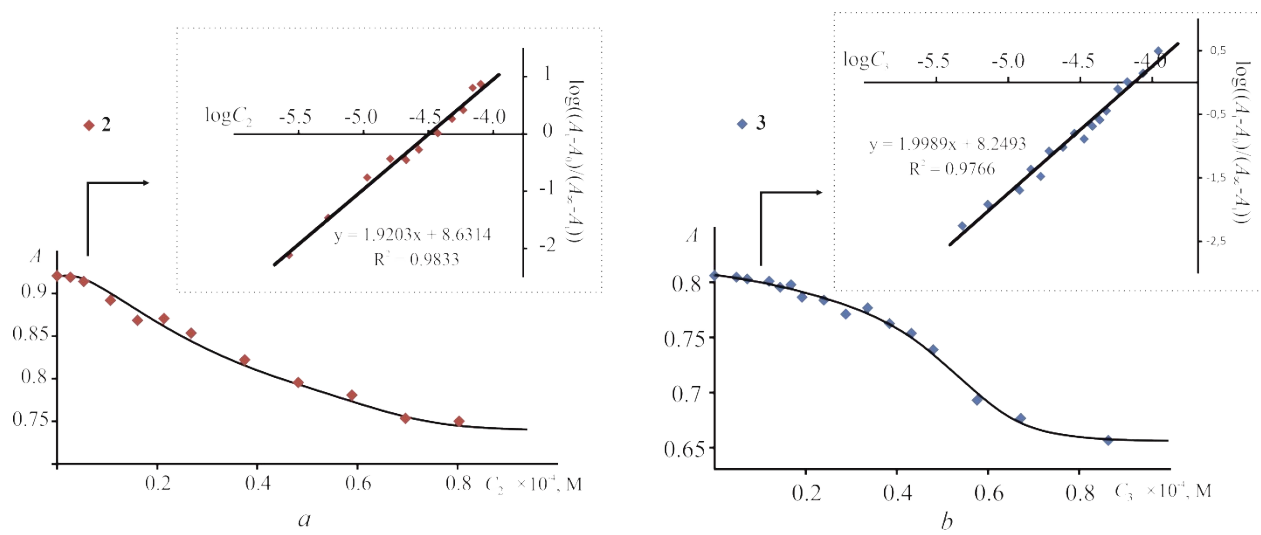


Fig. S7. The IR spectra of 1 and its dyad with 3 in KBr. Bands corresponding to vibrations of 3 are denoted with asterisks

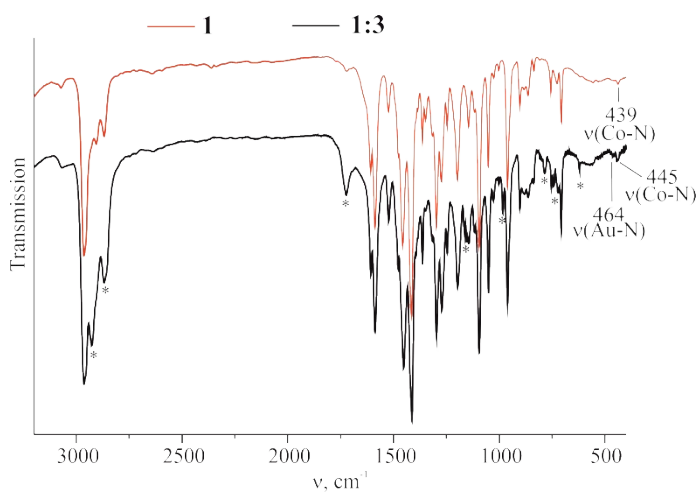
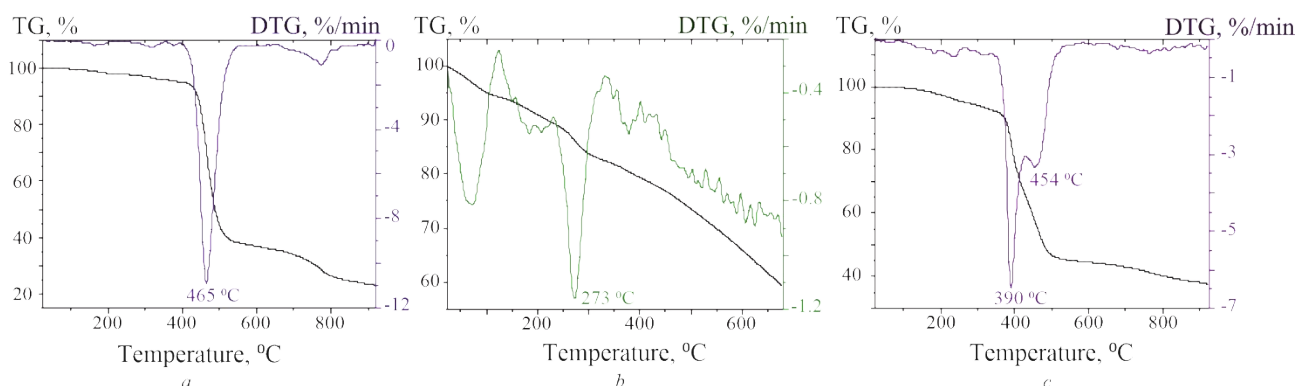


Table S2. The chemical shifts of protons of 1 and 1:2/1:3 dyad

Proton	1	1:3	1:2
H _{isoindole}	16.46 (s, 8H)	11.52	11.54
H _o	8.93 (s, 16H)	7.64	7.64
H _p	8.02 (s, 8H)	7.45	7.45
H _{tBu}	1.89 (s, 144H)	1.48	1.49
H _{meso}	-	10.67 (s, 2H) 10.54 (s, 1H)	10.68 (s, 1H) 10.56 (s, 2H)
H _{Py}	-	9.19 (m, 2H) 8.38 (s, 1H) 7.89 (s, 1H)	9.16 (br. s, 2H) 8.10 (m, 2H)
H _{CH2}	-	4.23 (s, 4H)	4.22 (s, 4H)
H _{CH3}	-	3.74 (m, 12H) 2.56 (s, 6H) 1.92 (s, 6H)	3.69 (m, 12H) 2.61 (s, 6H) 1.93 (m, 6H)

Fig. S8. TG and DTG curves for 1 (a), 3 (b) and 1:3 (c) powder from 25 °C to 920 °C, heating rate of 10 °C/min.

Thermal analysis (TG/DTG) of the complexes was carried out in argon using a Netzsch TG 209 F1 microthermal balance. The heating rate of the samples, sample weights and temperature range were 10 °C/min, 3.5-4.7 mg and 25-920 °C respectively. The resolution of microthermal balances is 1×10^{-4} mg.

Table S3. The peak potentials for 3, 2, 1:3, 1:2 in CH₂Cl₂ containing 0.1 M (n-Bu)₄NClO₄

Compound	Peak oxidation, V				Peak reduction, V		
3	1.58	1.13	-0.67	-1.34	1.5	-0.9	-1.44
2	1.60	1.14	-0.70	-1.34	1.5	-0.9	-1.43
1:3	1.60	0.64		-1.32	1.54	-0.93	-1.42
1:2	1.59	0.65		-1.32	1.53	-0.94	-1.43

Figure S9. The selective bond lengths (\AA) of 1, 2Cl, 3Cl. Hydrogen atoms are omitted for clarity

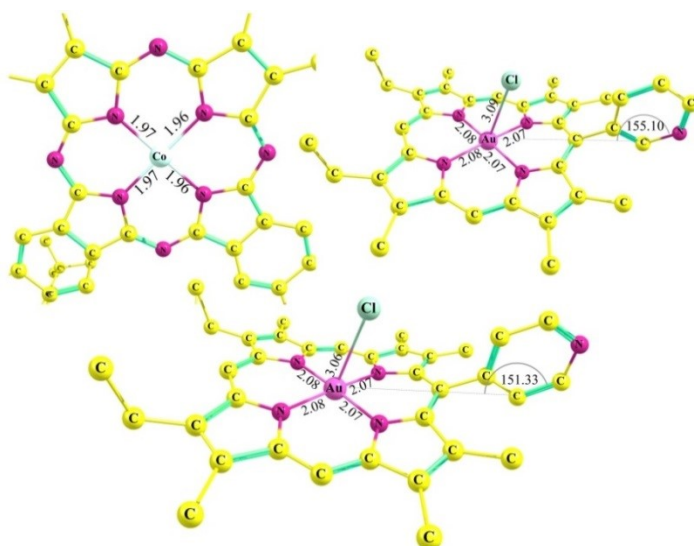
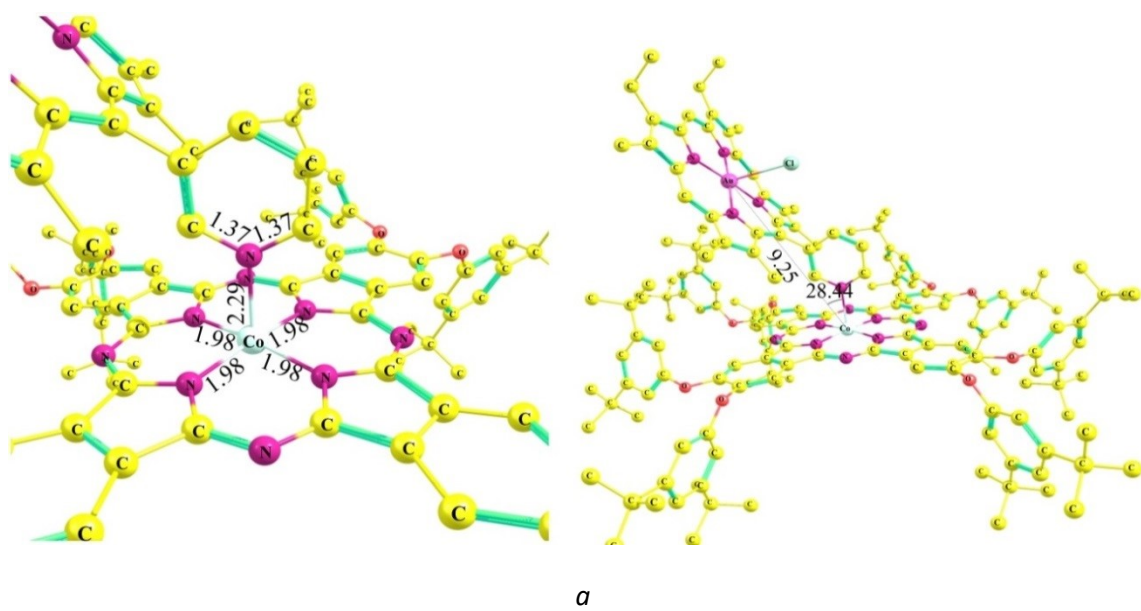
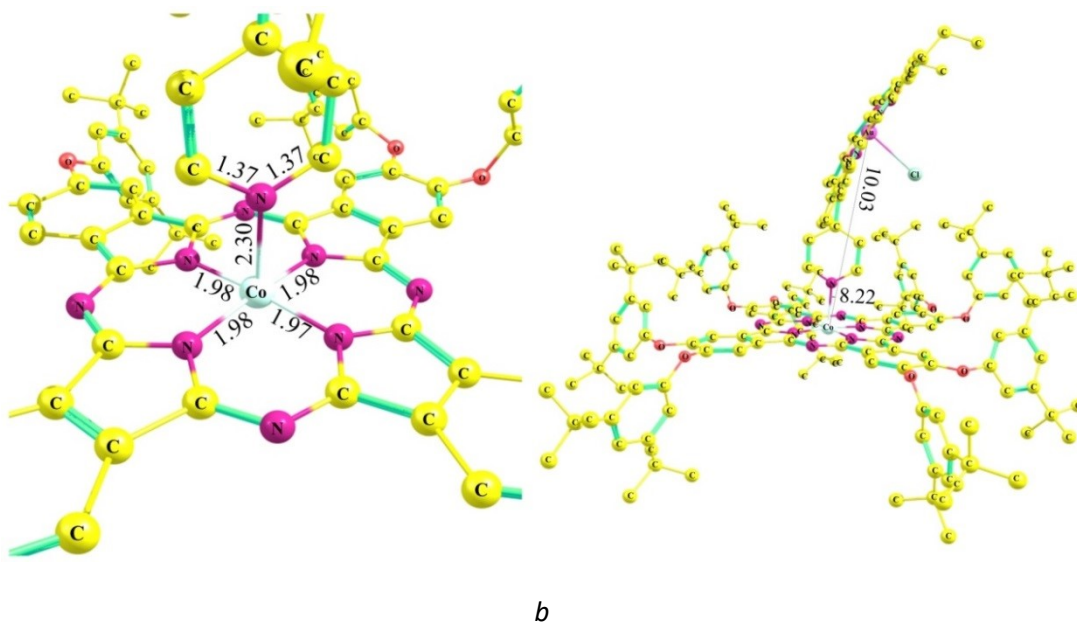


Figure S10. The selective bond lengths (\AA) of 1:3Cl (a) and 1:2Cl (b). Hydrogen atoms are omitted for clarity





b

Table S4. Bond order analysis based on Mulliken, Mayer, and Laplacian bond order of 2, 3 compounds

Bond	Mulliken bond order	Maer bond order	Laplacian bond order
2			
Au-N1	0.23324642	0.52090742	0.263458
Au-N2	0.23325256	0.52088947	0.263483
Au-N3	0.26067167	0.51422554	0.259339
Au-N4	0.26064704	0.51421629	0.259355
Au-Cl	0.33010934	0.51361085	0.067094
3			
Au-N1	0.23381338	0.52148728	0.264238

Au-N2	0.23380995	0.52148182	0.264240
Au-N3	0.26125646	0.51476734	0.260595
Au-N4	0.26125843	0.51476749	0.260593
Au-Cl	0.31448266	0.48674463	0.062604

Table S5. The conductivity and molar conductivity of 3 in CH₂Cl₂

	Conductivity (κ), mS/m	Molar conductivity (λ), S m ² /mol
CH ₂ Cl ₂	0.232	-
3 ($C = 1.7 \times 10^{-3}$ M)	4.697	2.763
(Cl)MnOEP* ($C = 1.86 \times 10^{-3}$ M)	0.203	0.109

*2,3,7,8,12,13,17,18-Octaethyl-21H,23H-porphine manganese(III) chloride

Figure S11. Energy diagrams of the frontier MO (alpha) levels and its shapes (Isodensity contour 0.03) for 1, 2Cl, 3Cl, 1:3Cl and 1:2Cl in toluene calculated using TD-UB3LYP*/6-31G (C, H, O, Cl) and Lanl2DZ (Co, Au) level of theory.

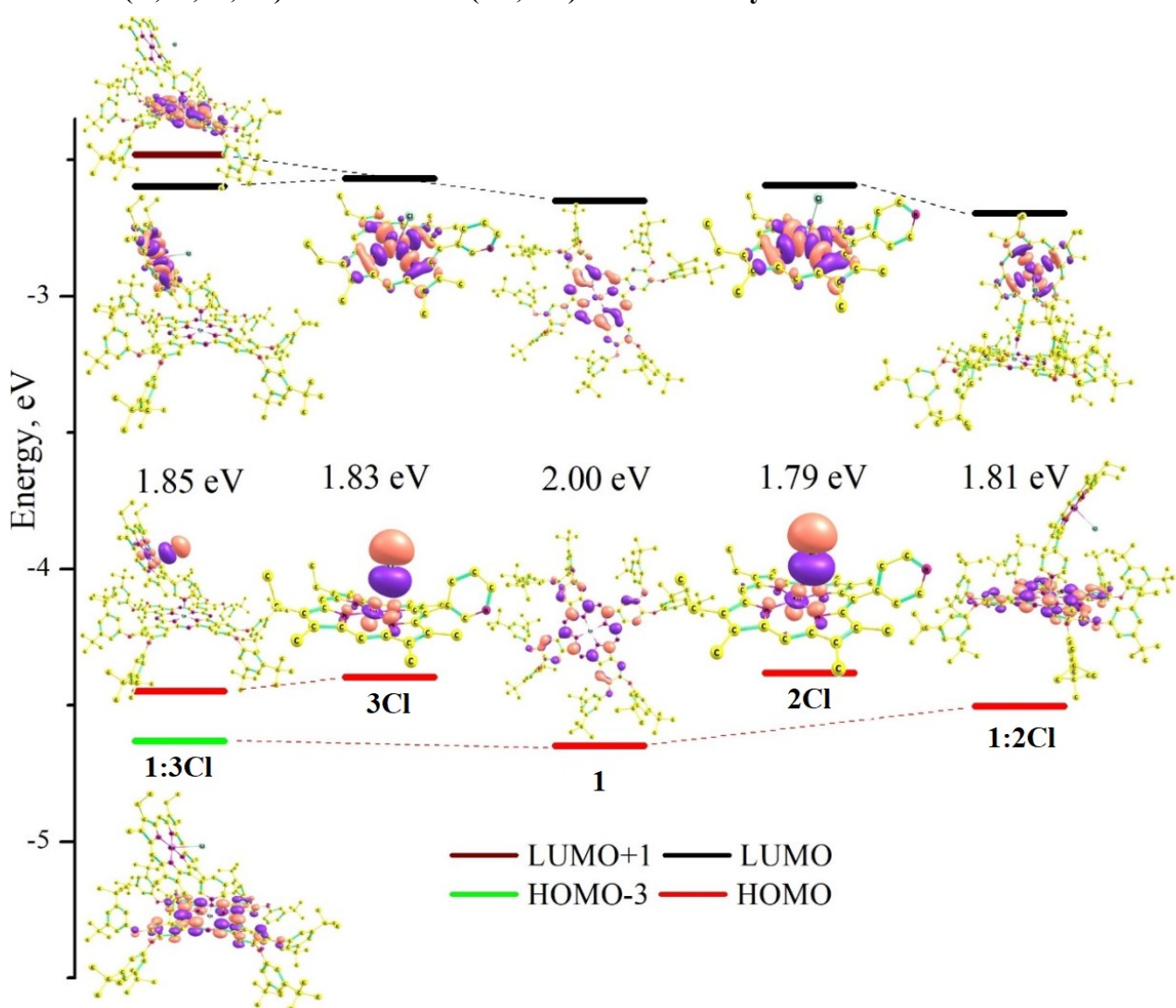


Table S6. The selected calculated optical transitions of 1:3 with oscillator strengths $f > 0.1$, wavelengths (nm) and main orbital transition contributions (>10%) of HOMO, LUMO (A- alpha orbitals, B – beta orbitals). Contour value is 0.03

Wavelength No.	Type of transaction	Contribution	
(nm)/Osc. strength			
46 637/0.458	HOMO(B)	LUMO+4(B)	43%
	HOMO(A)	LUMO+4(A)	38%
292 400/0.4359	HOMO-26(A)	LUMO+2(A)	34%
44 640/0.4043	HOMO(B)	LUMO+3(B)	31%
	HOMO(A)	LUMO+3(A)	28%

		H-21(A)	L+3(A)	15%
302	394/0.2241			
		H-21(A)	L+4(A)	21%
		H-21(B)	L+3(B)	22%
		H-21(B)	L+4(B)	27%
290	401/0.1784	H-26(A)	L+2(A)	52%

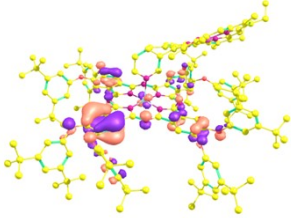
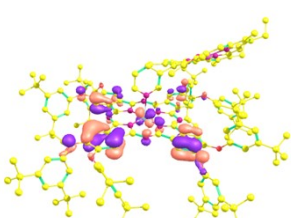
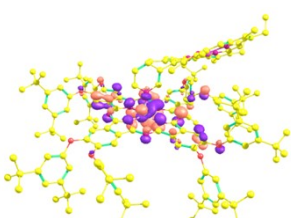
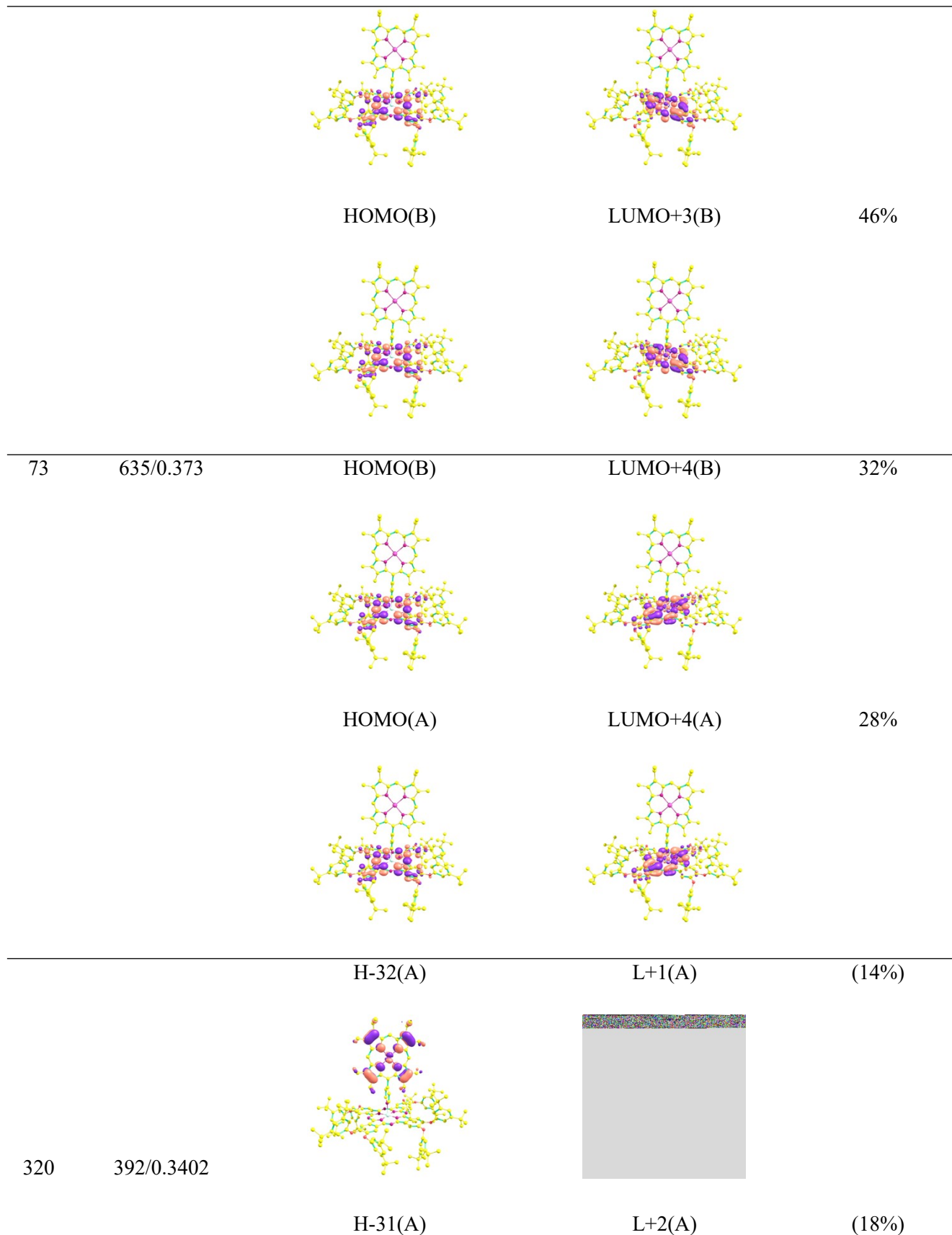
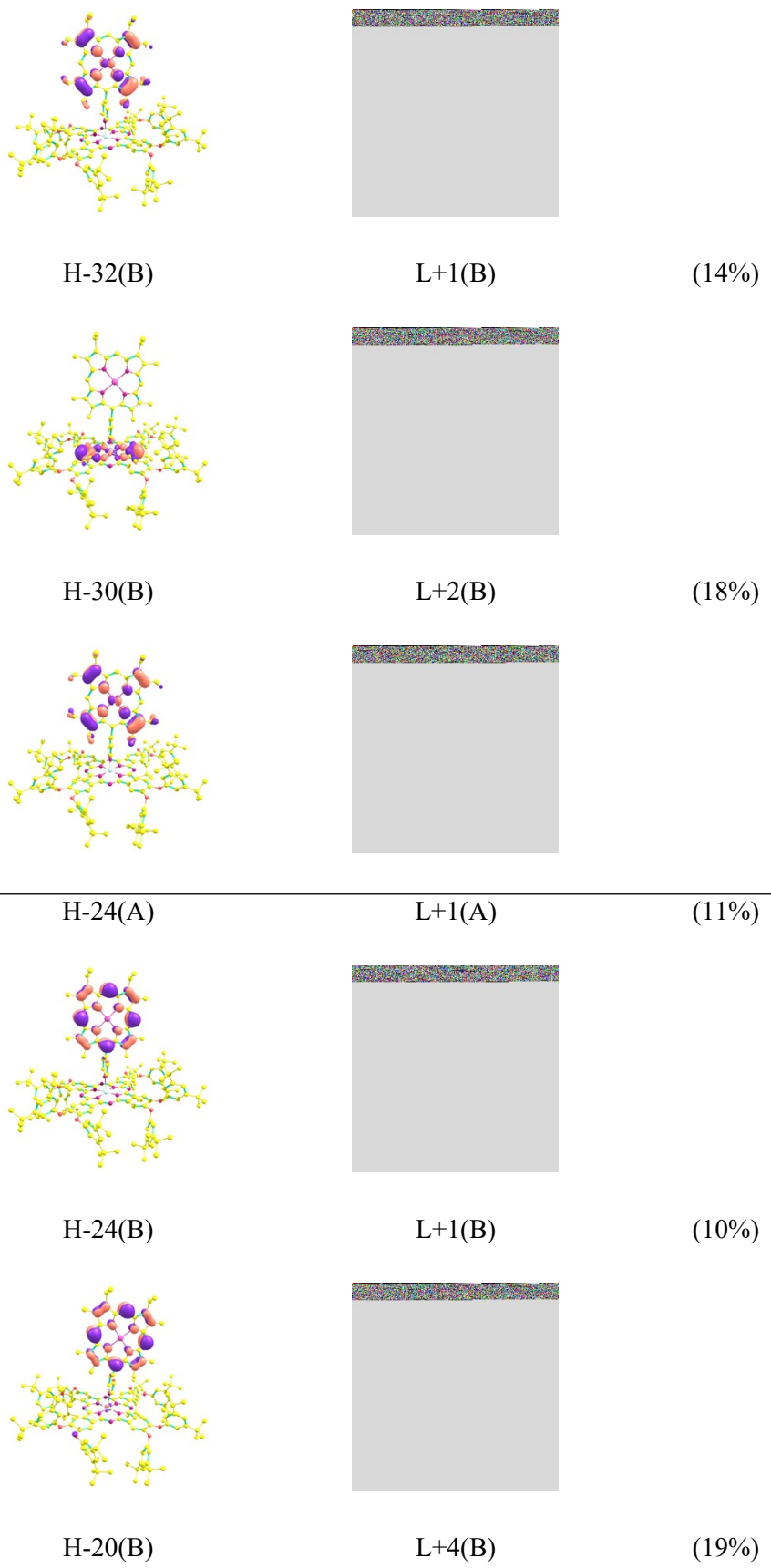
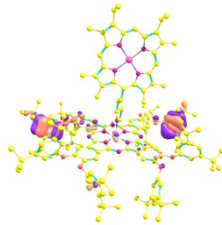
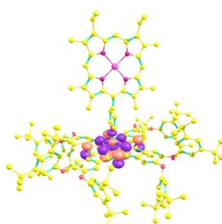
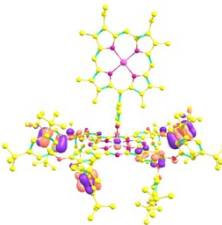
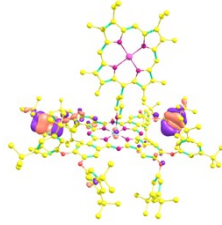
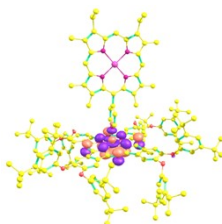
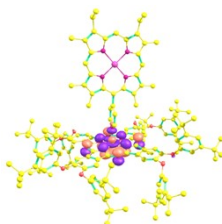
					
		H-21(A)	L+4(A)	13%	
297	397/0.1388				
		H-21(B)	L+3(B)	13%	
					
		H-27(B)	L+3(B)	18%	
364	357/0.1298				
		H-31(A)	L+4(A)	15%	
409	341/0.1158				

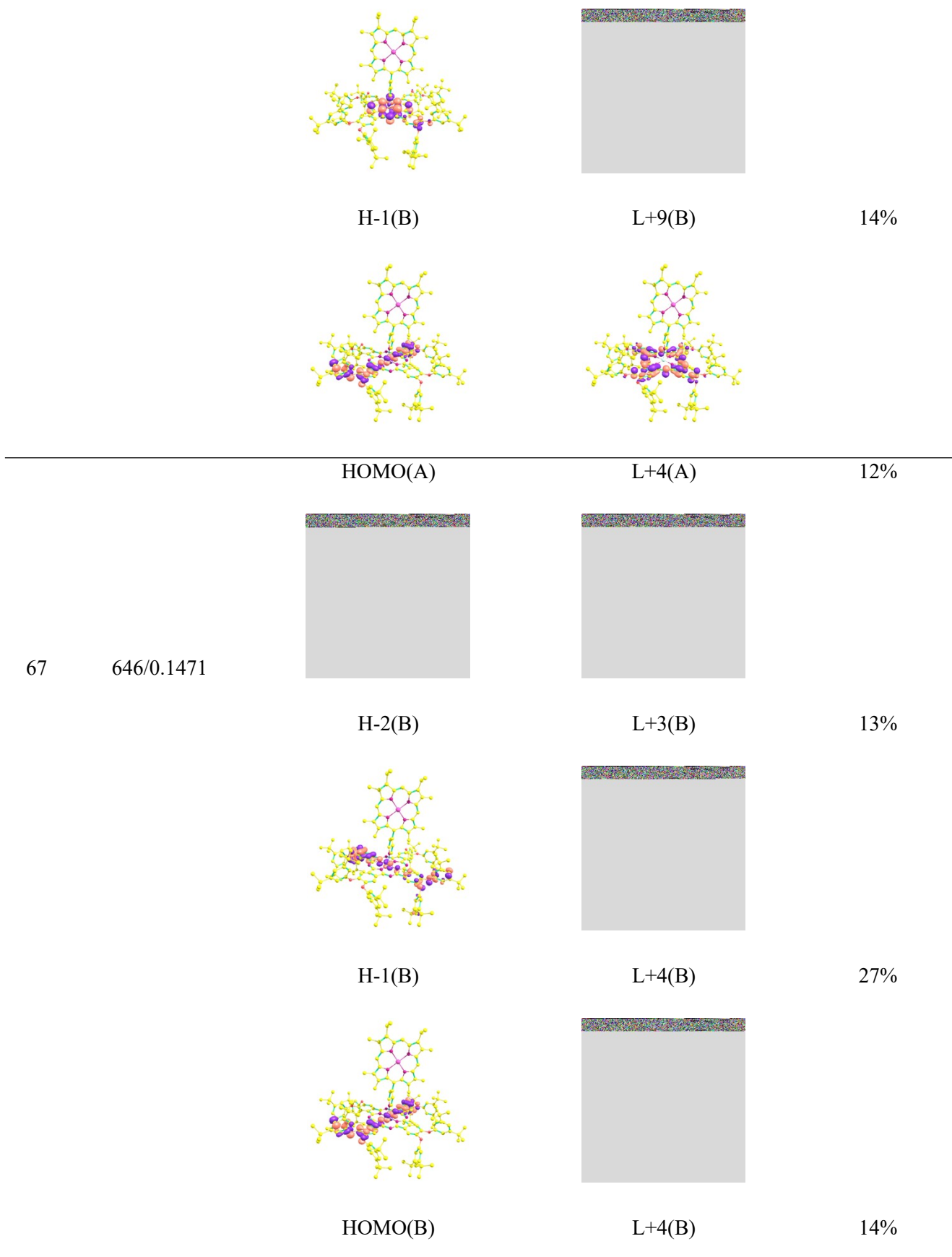
Table S7. The selected calculated optical transitions of 1:2 with oscillator strengths $f > 0.1$, wavelengths (nm) and main orbital transition contributions (>10%) of HOMO, LUMO. Contour value is 0.03

Wavelength No.	(nm)/Osc. strength	Type of transaction	Contribution	
312	396/1.2845	HOMO-24(A)	LUMO+2(A)	25%
		HOMO-22(A)	LUMO+1(A)	16%
		HOMO-24(B)	LUMO+2(B)	22%
		HOMO-22(B)	LUMO+1(B)	16%
70	641/0.5138	HOMO(A)	LUMO+3(A)	41%





			H-29(A)	L+2(A)	(14%)
315			394/0.252	L+4(A)	
			H-20(A)	L+4(A)	17%
			H-20(B)	L+4(B)	20%
			H-29(A)	L+4(A)	27%
441			340/0.1733	L+4(B)	10%
			H-26(B)		



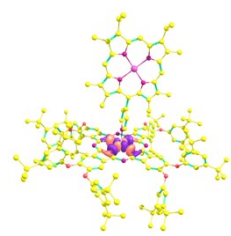
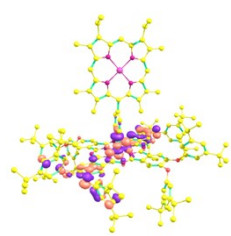
				
	H-29(A)		L+3(A)	17%
447	339/0.1387			
	HOMO(B)		L+15(B)	18%
				
	H-8(A)		L+3(A)	12%
219	450/0.1098			
	H-8(B)		L+3(B)	36%

Table S8. The selected calculated electron transitions, Λ parameters values and Δr -index for 1:2 and 1:3 by using B3LYP/6-31G level of theory with oscillator strengths $f > 0.05$

1:3				1:2			
Excited state	Λ	Δr -index, Å	Osc. Strength	Excited state	Λ	Δr -index, Å	Osc. Strength
46	0.657821	1.34	0.458	312	0.609933	1.33	1.2845
292	0.301628	6.12	0.4359	70	0.668205	0.50	0.5138
44	0.54977	3.00	0.4043	73	0.54873	1.76	0.373
293	0.467297	3.44	0.2564	320	0.617678	0.57	0.3402
299	0.461166	3.30	0.2519	313	0.495182	1.28	0.3248
294	0.443515	3.65	0.2472	315	0.343847	2.88	0.252
302	0.409089	4.58	0.2241	441	0.479576	2.00	0.1733
290	0.197004	7.63	0.1784	67	0.48483	1.30	0.1471
297	0.410349	3.97	0.1388	447	0.475519	1.35	0.1387
364	0.422103	4.24	0.1298	219	0.376564	2.12	0.1098
409	0.453967	2.44	0.1158	440	0.369574	1.12	0.0945
301	0.487109	3.20	0.0997	419	0.557762	1.40	0.0941
447	0.258815	7.76	0.0981	412	0.46127	1.95	0.0887
402	0.399063	4.58	0.0945	396	0.531323	2.04	0.0821
41	0.253995	9.22	0.0814	218	0.421349	2.28	0.081
306	0.377404	3.74	0.077	160	0.161225	4.49	0.0809
403	0.29218	6.18	0.0745	443	0.415374	2.07	0.0753
499	0.290221	5.80	0.0712	255	0.281141	3.59	0.075
417	0.486275	2.66	0.0708	163	0.315809	2.47	0.0708
455	0.301455	7.00	0.0677	414	0.51602	1.46	0.064
165	0.357453	4.04	0.0676	405	0.288897	3.10	0.0633
406	0.417262	2.51	0.0662	221	0.373709	2.89	0.0597
414	0.302066	5.97	0.0638	408	0.379867	1.86	0.0579
42	0.176147	11.57	0.0618	497	0.460322	3.53	0.0541
155	0.38648	3.87	0.0617	403	0.393642	2.44	0.0505
373	0.449761	3.43	0.0613				
269	0.321665	4.70	0.0608				
313	0.226602	7.33	0.0589				

389	0.385988	3.63	0.0556				
199	0.360577	4.10	0.0528				
360	0.480432	3.41	0.0511				

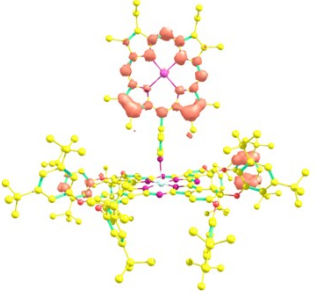
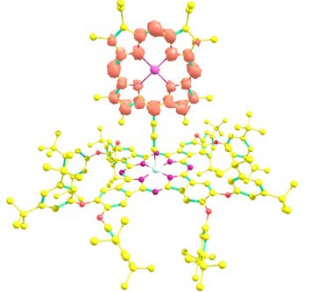
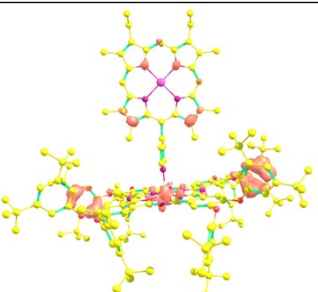
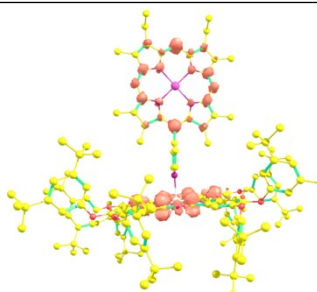
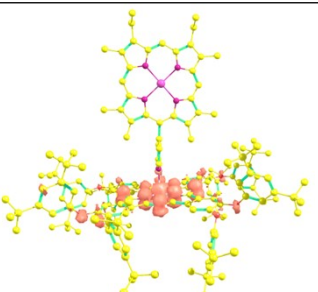
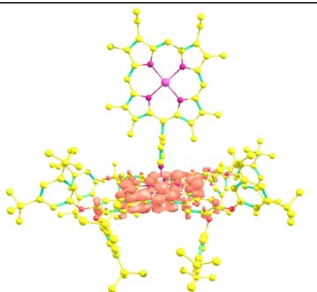
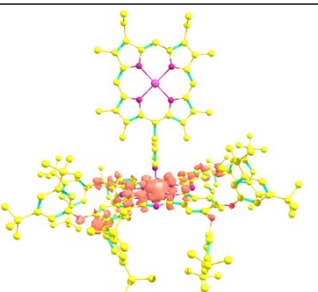
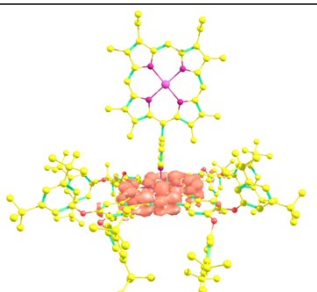
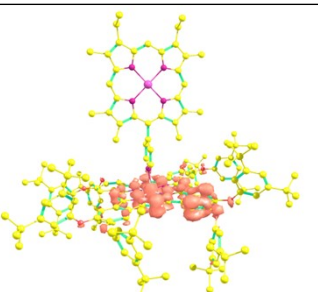
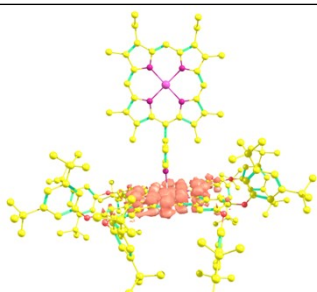
Table S9. The Natural Transition Orbitals of 1:3 for electron excitation with oscillator strengths $f > 0.1$, wavelengths (nm) and main orbital transition contributions (>10%). A - alpha orbitals, B – beta orbitals. Contour value is 0.001

	Hole	Electron	Composition Hole	Composition Electron
S46			HOMO (A) (39 %) HOMO (B) (43 %)	LUMO+4 (A) (38 %) LUMO+4 (B) (47 %)
S29 2			HOMO-26 (A) (35 %)	LUMO+2 (A) (14 %) LUMO+3 (A) (49 %) LUMO+1 (B) (14 %) LUMO+2 (16 %)
S44			HOMO (A) (30 %) HOMO (B) (33 %)	LUMO+3 (A) (30 %) LUMO+3 (B) (43 %)
S30 2			HOMO-21 (A) (36 %) HOMO-21 (B) (50 %)	LUMO+3 (A) (18 %) LUMO+4 (A) (24 %) LUMO+3 (B) (23 %) LUMO+4 (B) (29 %)

S29 0		HOMO-26 (A) (52 %)	LUMO+2 (A) (68 %) LUMO+2 (B) (14 %)
S29 7		HOMO-21 (A) (19 %) HOMO-21 (B) (13 %)	LUMO+4 (A) (25 %) LUMO+3 (B) (20 %)
S36 4		HOMO-27 (B) (23 %)	LUMO+3 (A) (28 %) LUMO+3 (B) (20 %) LUMO+4 (B) (15 %) LUMO+6 (B) (15 %)
S40 9		HOMO-31 (A) (18 %)	LUMO+4 (A) (13 %) LUMO+5 (A) (33 %) LUMO+3 (B) (26 %) LUMO+4(B) (14 %)

Table S10. The Natural Transition Orbitals of 1:2 for electron excitation with oscillator strengths $f > 0.1$, wavelengths (nm) and main orbital transition contributions (>10%). A – alpha orbitals, B – beta orbitals. Contour value is 0.001

	Hole	Electron	Composition Hole	Composition Electron
S312			HOMO-22 (A) (24 %) HOMO-22 (B) (22 %) HOMO-24(B) (16 %) HOMO-24 (A) (16 %)	LUMO+1 (A) (17 %) LUMO+2 (A) (25 %) LUMO+1 (B) (17 %) LUMO+2 (B) (25 %)
S70			HOMO (A) (41 %) HOMO (B) (46 %)	LUMO+3 (A) (40 %) LUMO+3 (B) (51 %)
S73			HOMO (A) (29 %) HOMO-5 (B) (11 %) HOMO (B) (32 %)	LUMO+4 (A) (30 %) LUMO+5 (B) (14 %) LUMO+4 (B) (41 %)
S320			HOMO-32 (A) (14 %) HOMO-31 (A) (18 %) HOMO-32 (B) (14 %) HOMO-30 (B) (18 %)	LUMO+1 (A) (23 %) LUMO+2 (A) (25 %) LUMO+1 (B) (23 %) LUMO+2 (B) (25 %)

S313			HOMO-21 (A) (11 %) HOMO-24 (B) (10 %) HOMO-20 (B) (21 %)	LUMO+1 (A) (15 %) LUMO+2 (A) (14 %) LUMO+1 (B) (16 %) LUMO+2 (B) (14 %) LUMO+4 (B) (22 %)
S315			HOMO-29 (A) (14 %) HOMO-20 (A) (20 %) HOMO-20 (B) (21 %)	LUMO+2 (A) (20 %) LUMO+4 (A) (22 %) LUMO+4 (B) (23 %)
S441			HOMO-29 (A) (28 %) HOMO-26 (B) (11 %) HOMO-1 (B) (14 %)	LUMO+4 (A) (32 %) LUMO+4 (B) (17 %) LUMO+9 (B) (17 %)
S67			HOMO (A) (13 %) HOMO (B) (15 %) HOMO-1 (B) (29 %) HOMO-2 (B) (14 %)	LUMO+4 (A) (15 %) LUMO+3 (B) (22 %) LUMO+4 (B) (52 %)
S447			HOMO-29 (A) (18 %) HOMO (B) (120 %)	LUMO+3 (A) (20 %) LUMO+4 (15 %) LUMO+3 (B) (13 %) LUMO+4 (B) (14 %) LUMO+15 (B) (19 %)

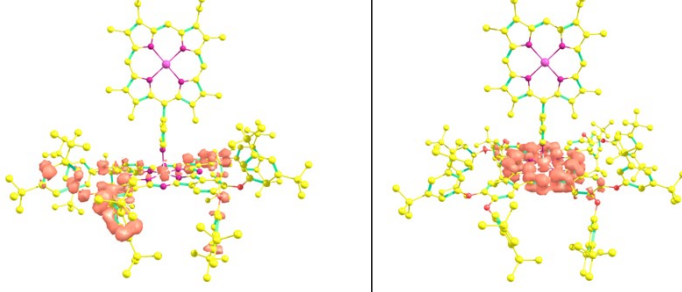
S219		HOMO-10(A) (11 %) HOMO-8 (A) (15 %) HOMO-8 (B) (42 %)	LUMO+3 (A) (29 %) LUMO+4 (A) (12 %) LUMO+3 (B) (38 %) LUMO+4 (B) (20 %)
------	---	--	--

Figure S12. The femtosecond transient absorption spectra of **1** at the excitation wavelength of 400 nm in argon saturated 1,2- dichlorobenzene at indicated time intervals.

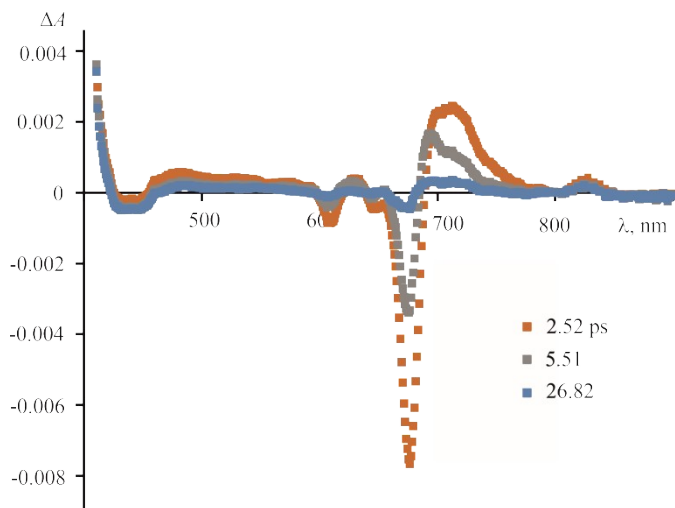


Figure S13. The femtosecond transient absorption spectra of **2** at the excitation wavelength of 400 nm in argon saturated 1,2- dichlorobenzene at indicated time intervals.

